COMPUTERS AND BIOMEDICAL RESEARCH 14, 19–30 (1981)

A Computer Aided Simulation of an Electrode Penetration into Deep Brain Structures

YEHEZKEL YESHURUN, NACHUM ALLON, AND ZVI WOLLBERG

Department of Mathematical Sciences, Division of Applied Mathematics, and Department of Zoology, George S. Wise Faculty of Life Sciences, Tel Aviv University, Tel Aviv, Israel

Received May 14, 1979

An interactive computer graphics program has been designed for simulating the penetration of a microelectrode into the medial geniculate body (MGB) model of the squirrel-monkey. This program enables us to obtain a perspective 3-D plot of the MGB model, viewed from any selected spatial point and to reconstruct from it sections in any plane. A preselected or reconstructed penetration tract can thus be graphically described, superimposed on any selected plane which contains the electrode. The program can be used on line, when fast selection or reconstruction of a probe location is required under surgical or experimental conditions.

INTRODUCTION

Probing into deep brain structures for surgery or neurophysiology is performed routinely with stereotaxic frames and atlases. The brain sections from which such atlases are constructed are usually in coronal, sagittal and horizontal planes. It is relatively easy to direct a probe with considerable accuracy into a deep structure, when the penetration tract parallels at least one plane in the atlas. However, when the penetration tract has to be interpolated from two adjacent sections, difficulties arise in visualizing the position of the probe relative to the various brain structures. The difficulty becomes even greater when the tract is oblique to all three stereotaxic planes. Individual variability in size and location of deep brain structures, relative to standard coordinates of the atlas, presents additional difficulties in guiding the electrode precisely towards a definite target. These difficulties can be overcome by manual calculations, combining the use of stereotaxic atlases, various roentgenological and electrophysiological techniques, and mathematical manipulations. However, such procedures are burdensome and time-consuming when executed manually. They cannot be used as routine procedures when fast selection or reconstruction of a probe location is required under surgical or experimental conditions.

We are currently studying the response properties of single cells in the medial geniculate body (MGB)—a thalamic auditory nucleus—in the awake and undrugged squirrel monkey (*Saimiri sciureus*). Repeated recordings are

0019-9958/81/010019-12$02.00/0

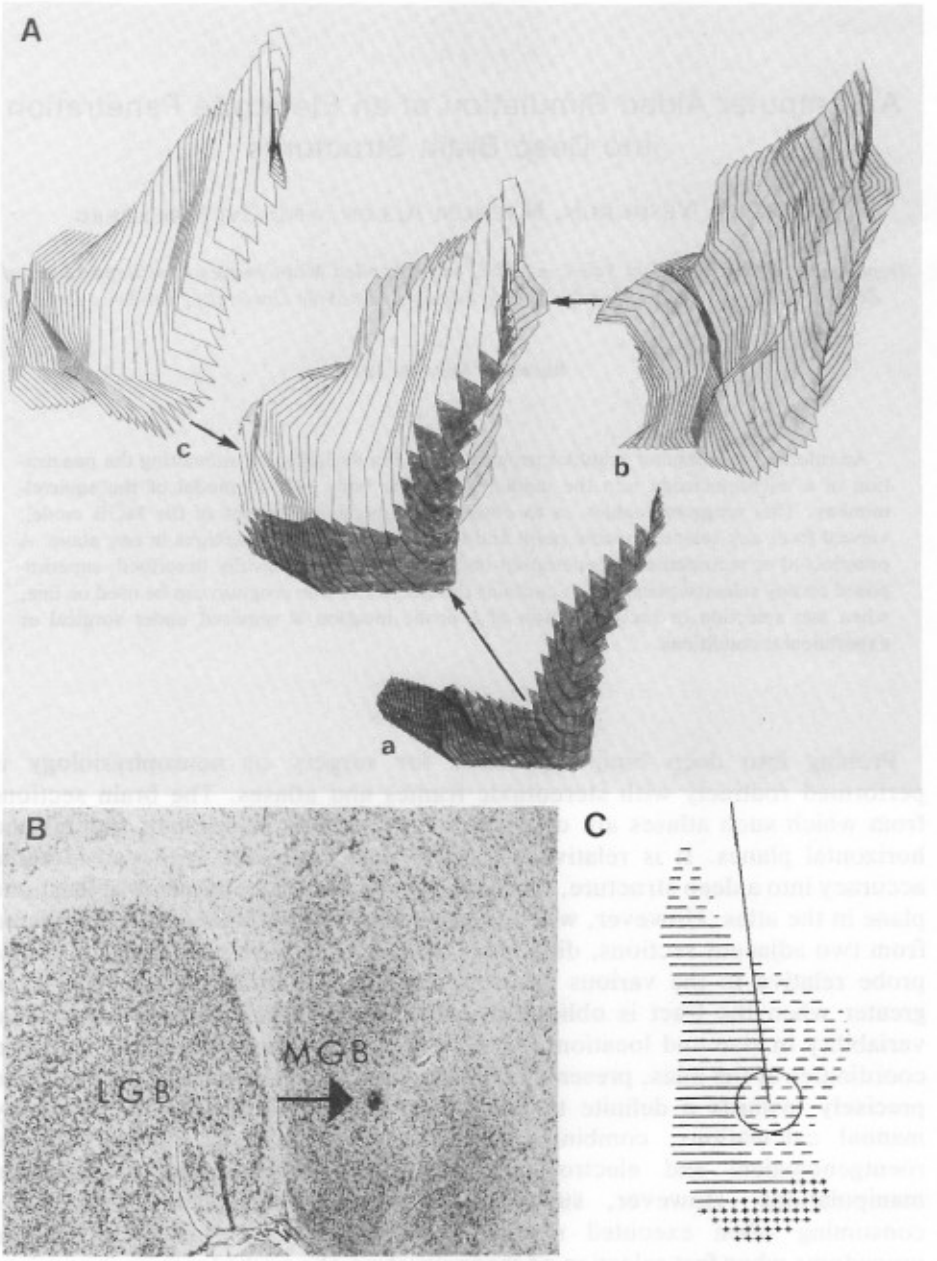

FIG. 1. An illustration of the simulated medial geniculate body (MGB) and of a reconstructed electrode plane. (A) An antero-lateral view of the simulated MGB illustrating the shape and spatial organization of its three subdivisions a, b and c. (B) A photomicrograph of a coronal section through the MGB. The arrow points to a marking lesion. The borderlines of the MGB (specially in its medial aspect) and its subdivisions are not clearly visible in a single histological section, but can

made from the same monkey for several months, and in order to avoid the use of a stereotaxic frame, we implant a Plexiglas cylinder above an aperture drilled in the skull of the monkey (the base of the cylinder is denoted hereafter as the "manipulator plane").

During recording sessions the cylinder carries a calibrated manipulator which allows the insertion of a microelectrode to any desired depth at any point on the exposed brain. Marking lesions are made only at the end of the last recording session. With this approach the monkey sits in a chair in relative comfort during the experiment, able to move all parts of its body except the head. Details concerning the operation procedures are described in earlier works (*1, 2*).

The MGB is a deep brain structure (relatively small in the squirrel monkey), which can be further divided histologically (*3, 4*), and physiologically (*5*), into three major subdivisions. Thus any minor deviation in the implantation of the cylinder from standard coordinates requires compensatory corrections when preselecting or reconstructing electrode tracts. This and all the aforementioned difficulties, arising when a quick decision has to be made concerning the spatial location of an electrode, led us to design an interactive computer graphics program and integrate it into our experimental setup. This program provides a perspective 3-D plot of a model of the structure under study viewed from any given spatial point. It also allows the reconstruction of sections of the model in any desired plane. A preselected or reconstructed electrode tract can thus be graphically described, superimposed on any selected plane which contains the electrode (Fig. 1). This program is, in this regard, complementary to earlier computational techniques, designed mainly for neurosurgical purposes (e.g., *6–9*).

Although the program was tailored for a particular brain structure in a specific animal species, it can be applied to all brain structures in any species.

In what follows we discuss both the mathematical principles of the program and its application. First we present the structure of the coordinate file containing the spatial coordinates of a given solid body, and then we describe the process of obtaining such coordinates of the MGB.

The logic and the flow of the program are discussed in detail, followed by a description of its use.

Hardware and Auxiliary Software

The program is executed on the CDC-6600 computer of the Tel Aviv University under NOSBE 1.2 operating system, and is written in Fortran IV. A

---

be defined by a series of sections (see also 4), on which we based our digitized data (*3, 10*) (C) A computer reconstruction of the same section illustrating the electrode tract and the location of the lesion (centre of the circle). The diameter of the circle represents an estimated range of error (discussed in the text). The three different subdivisions of the MGB, a, b, c are designated by the crosses, dashed lines and solid lines, respectively.

Tektronix 4010-1 or a DEC GT-42 graphic display terminal is used for interactive processing and display. Hard copies of the drawings are available by using a CALCOMP 565 plotter. The graphical output of the program can be displayed by any of the above mentioned devices, since the graphics package (GD3) produces a device independent display file.

Coordinate File Structure

The file consists of the spatial coordinates (X_i, Y_i, Z_i) of a set of points, which constitutes, when properly connected, the contour lines of a solid 3-D body. This set of points is divided into several blocks, each block including points sharing a common Z coordinate, and thus comprising a cross section. The points of each cross section are clockwise (or counterclockwise) ordered, and the last one coincides with the first one, so that a closed contour is formed if a line is passed through all the points. This line can be constructed by means of interpolation. Without a loss of generality, we shall restrict ourselves to piecewise linear interpolation.

If the solid body includes several subdivisions, we then further define several records in each block, where each record represents a polygon. This polygon is the contour line of the corresponding subdivision in the corresponding cross section.

The number of points in each record (subdivisions) remains fixed through all the blocks (cross sections). This requirement is mandatory, since we assume that the point p_j at block i, is "connected" to the point p_j at block $i + 1$. By this assumption, we are able to reconstruct any required cross section between two given cross sections i and $i + 1$, by means of interpolation (Fig. 2).

Determination of the Actual Coordinates

The MGB of the squirrel monkey consists of three divisions (following the terminology and the division of Jordan (*3*)). Each subdivision's contours are defined on a series of frontal sections with known stereotaxic coordinates (*10*). We define the cartesian coordinate system as follows (Fig. 4): X-left-right (=

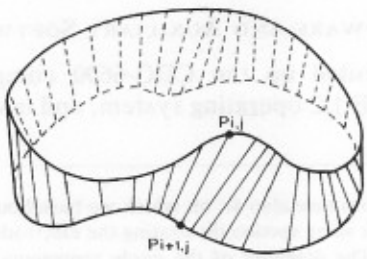

FIG. 2. Method for pairing two consecutive cross sections. P_{ij} and $P_{i+1,j}$ are the points P_j of blocks i and $i + 1$, respectively.

lateral) axis, right is positive. *Y*—ventral-dorsal (= vertical) axis, dorsal is positive. *Z*-posterior-anterior axis, anterior is positive. The origin (0, 0, 0) coincides with the origin of the atlas (*10*).

The contour lines of a certain subdivision in each section are approximated by A polygon. The number of the polygon vertices is determined as the minimal number so that the polygon's contour is as close as possible, subjectively judged, to the substructure's outline. Since each of the three subdivisions must have a fixed number of vertices, N_1, N_2, N_3, respectively, through all the cross sections, these numbers are determined by consulting the cross section where the corresponding subdivision contour is longest and most winding. The number of vertices actually chosen was $N_1 = 9$, $N_2 = 18$, $N_3 = 26$ for the three subdivisions (Fig. 3). In a cross section where a certain subdivision does not exist, all the points of the corresponding block degenerate into one subjectively selected point.

Having all the cross sections and substructures digitized, we now correlate the respective vertex p_j of any two adjacent cross sections so that the 3-D body obtained by connecting these points resembles, as much as possible, the original MGB. This task is aided by producing 3-D perspective views of the body.

This process of pairing the vertices subjectively, although somewhat tedious, was found to yield superior results to some automatically programmed pairing techniques we tried. It should also be kept in mind that this process is carried out only once. A recently suggested algorithm, not yet tried by us, provides a programmed solution for the pairing problem (*9*).

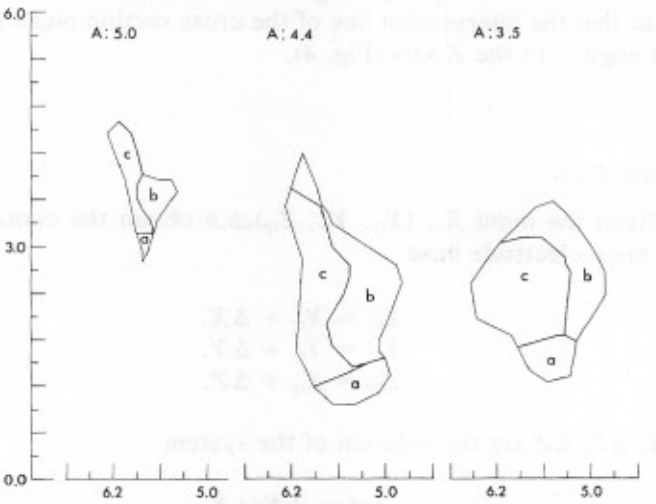

FIG. 3. A computer reconstruction of three different coronal sections, illustrating the three subdivisions a, b, c. The *Y* and *X* axes represent the vertical and lateral coordinates according to the sterotaxic atlas of Emmers and Akert (*10*). The number above each section designates the location of the section along the anterior-posterior axis. Scale in millimeters.

Program Logic and Flow

(a) *Preliminary Considerations*

A reference microelectrode is driven into the brain. This electrode is characterized by its tip distance (R_r) from the manipulator plane; by its tip coordinates (X_{tr}, Y_{tr}, Z_{tr}); by the angle between its projection on the $X = 0$ plane and the Y axis (θ); and by the angle between its projection on the $Z = 0$ plane and the Y axis (ϕ). ϕ and θ are restricted to $[-90°, 90°]$. We refer to these specific angles, since they are obtained from a roentgenographic display (Fig. 4).

The intersection point of the reference electrode and the manipulator plane (the electrode base) is defined to be the origin (0, 0) of a cartesian coordinate system on this plane. The axis of the manipulator plane denoted U is chosen to be parallel to the $Z = 0$ plane (i.e., moving along the U axis does not change the Z-coordinate). The other axis is denoted V.

The electrode base can afterwards be shifted on the manipulator plane, but the electrode is always normal to this plane.

The program is usually operated as follows: The user enters R_r, (X_{tr}, Y_{tr}, Z_{tr}), ϕ and θ. The program uses these parameters to evaluate the micromanipulator position.

Then the user enters a pair (u, v) which designates the location of the base of a microelectrode on the manipulator plane, its length, R, and an angle $0 < \gamma < 180°$. The output of the program is a plot of a cross section through the simulated MGB. The cross section resides in a plane which contains the microelectrode. The remaining degree of freedom is satisfied by the requirement that the intersection line of the cross section plane and the $Y = 0$ plane is at angle γ to the Z axis (Fig. 4).

(b) *Program Flow*

1.1 Given the input R_r, (X_{tr}, Y_{tr}, Z_{tr}),ϕ,θ obtain the coordinates of the reference microelectrode base

$$\begin{aligned} X_{br} &= X_{tr} + \Delta X, \\ Y_{br} &= Y_{tr} + \Delta Y, \\ Z_{br} &= Z_{tr} + \Delta Z, \end{aligned} \qquad [1]$$

where ΔX, ΔY, ΔZ are the solution of the system

$$\begin{aligned} tg\phi &= \Delta X/\Delta Y \\ tg\theta &= \Delta Z/\Delta Y \\ \Delta x^2 + \Delta Y^2 + \Delta Z^2 = R_r^2 \rightarrow \Delta Y &= \left[\frac{R_r^2}{1 + tg^2\phi + tg^2\theta}\right]^{1/2}. \end{aligned} \qquad [2]$$

For the sake of covenience we now define θ' as the angle between the reference electrode and its projection on the $Z = 0$ plane:

$$\theta' = \arcsin \Delta Z / R_r \qquad [3]$$

such that ϕ and θ' are consistent with polar coordinate notation.

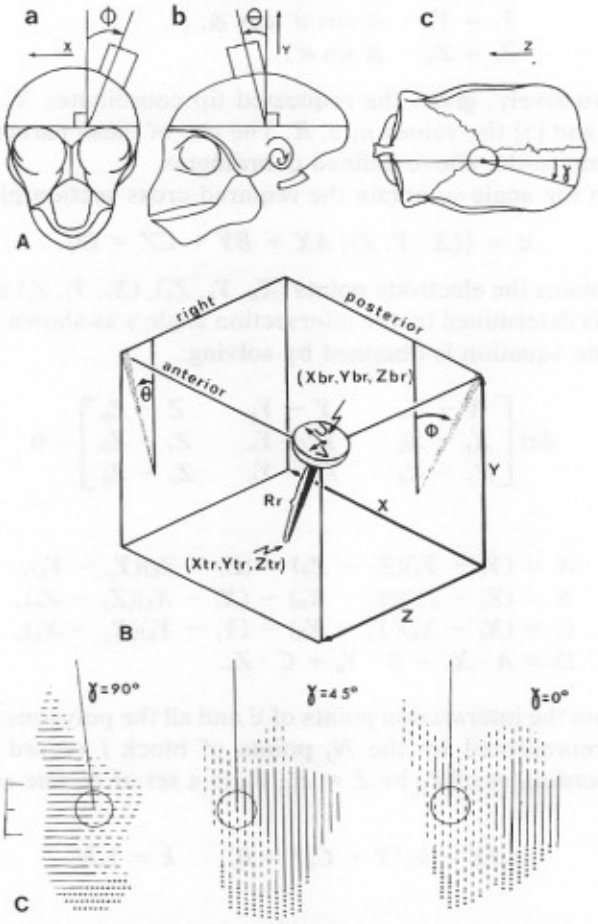

FIG. 4. Illustration of the various parameters which define the spatial microelectrode position. (A) Ink tracing of three X-ray views of the monkey's head. The frontal (a) and lateral (b) views illustrate ϕ and θ. The top view (c) demonstrates the user defined angle γ, which is the angle between the intersection line of the requested cross section plane and the $Y = 0$ plane, and the Z axis. The arrows marked X, Y and Z are in the corresponding axes directions (see B) (B) X, left right (= lateral) axis; Y, ventral dorsal (= vertical) axis; Z, posterior anterior axis. Characterization of the reference microelectrode: base at X_{br}, Y_{br}, Z_{br}; tip at X_{tr}, Y_{tr}, Z_{tr}; length, R_r. Axes of the cartesian coordinate system on the manipulator plane are U, V. (C) A computer reconstruction of a certain microelectrode tract within the MGB model superimposed on three different planes defined by three different γ values. Scale; 0.7 mm Subdivisions and meaning of circle as in Fig. 1.

2.1. Given a shift on the manipulator plane (u,v) and an electrode length R, calculate the base [4] and tip [5] coordinates of the electrode:

$$\begin{aligned} X_b &= X_{br} - v \sin\theta' \sin\phi + u \cos\phi; \\ Y_b &= Y_{br} - v \sin\theta' \cos\phi - u \sin\phi; \\ Z_b &= Z_{br} + v \cos\theta'; \end{aligned} \qquad [4]$$

$$\begin{aligned} X_t &= X_b - R \cos\theta' \sin\phi; \\ Y_t &= Y_b - R \cos\theta' \cos\phi; \\ Z_t &= Z_b - R \sin\theta'. \end{aligned} \qquad [5]$$

2.2. Alternatively, given the requested tip coordinates X_t, Y_t, Z_t, obtain from Eqs. [4] and [5] the values u, v, R. The use of these parameters will lead the electrode tip to the above defined coordinates.

3.1 Given the angle γ, obtain the required cross section plane equation

$$\mathfrak{P} = \{(X, Y, Z) \mid AX + BY + CZ = D\}. \qquad [6]$$

This plane contains the electrode points (X_b, Y_b, Z_b), (X_t, Y_t, Z_t) and a point (X_c, Y_c, Z_c) which is determined by the intersection angle γ as shown in Table I. The requested plane equation is obtained by solving:

$$\det\begin{bmatrix} X - X_b & Y - Y_b & Z - Z_b \\ X_t - X_b & Y_t - Y_b & Z_t - Z_b \\ X_c - X_b & Y_c - Y_b & Z_c - Z_b \end{bmatrix} = 0 \qquad [7]$$

which yields

$$\begin{aligned} A &= (Y_t - Y_b)(Z_c - Z_b) - (Z_t - Z_b)(Y_c - Y_b), \\ B &= (Z_t - Z_b)(X_c - X_b) - (X_t - X_b)(Z_c - Z_b), \\ C &= (X_t - X_b)(Y_c - Y_b) - (Y_t - Y_b)(X_c - X_b), \\ D &= A \cdot X_b + B \cdot Y_b + C \cdot Z_b. \end{aligned} \qquad [8]$$

4.1. Obtain the intersection points of $\mathfrak{P}$ and all the polygons: Let P_{ij} denote the polygon represented by the N_j points of block i record j, and let the common Z coordinates of P_{ij} be $Z = Z_s$. P_{ij} is a set of N_j line segments of the form

$$a_{ij}{}^k X + b_{ij}{}^k Y + C_{ij}{}^k = 0, \qquad k = 1, N_j. \qquad [9]$$

TABLE I

DEFINITION OF THE POINT (X_c, Y_c, Z_c) FOR DIFFERENT γ VALUES

	$\gamma \neq 0, 90, 180$	$\gamma = 0, 180$	$\gamma = 90$
X_c	$X_t + 1$	X_t	$X_t + 1$
Y_c	Y_t	Y_t	y_t
Z_c	$Z_t + 1/\mathrm{tg}\gamma$	$Z_t + 1$	Z_t

The intersection points of these line segments and $\mathfrak{L}$ are calculated by solving the linear systems

$$\begin{aligned} &AX + BY + CZ_s - D = 0, \\ &a_{ij}{}^k X + b_{ij}{}^k Y + c_{ij}{}^k = 0, \qquad k = 1,N_j \end{aligned} \tag{10}$$

Notice that we are able to determine the intersection points of $\mathfrak{L}$ with any polygon P which resides between the given polygons P_{ij} and $P_{i+1,j}$ since the vertices of P might be deduced by interpolation. Thus, we are able to obtain the intersection points of $\mathfrak{L}$ and the solid body in any required resolution.

5.1. Draw the cross section: Having the system [10] solved for $K = 1, N_j$, we obtain an even number of points (X_i, Y_i), $i = 1,m$: for if we do not consider a tangency point as an intersection point, a straight line "entering" a polygon must also "come out."

The points (X_i, Y_i), $i = 1,m$ share a common Z coordinate Z_s. We transform the point (X_i, Y_i, Z_s) to its coordinates in the section plane as follows:

$$\begin{aligned} H_i &= ((X_i - D1)^2 + (Y_i - D2)^2)^{1/2}, \\ T &= Z_s/\sin\beta \end{aligned} \tag{11}$$

where

$$\begin{aligned} D1 &= \frac{D - C \cdot Z_s}{B \cdot E}, \\ D2 &= \frac{D - C \cdot Z_s}{A \cdot E}, \\ E &= \frac{A^2 + B^2}{A \cdot B}, \\ \beta &= \operatorname{arctg} \frac{A + \mathrm{B}^2/A}{(-C)(1 + B^2/A^2)^{1/2}}. \end{aligned} \tag{12}$$

We now sort the points (H_i,T) by their H values, and draw at the display vertical coordinate T segments

$$(H_i, H_{i+1}), \qquad i = 1, 3, 5, \ldots, m - 1.$$

The electrode itself is drawn as a line segment between the points (X_b, Y_b, Z_b) (X_t, Y_t, Z_t) after similar transformation to (H, T) coordinates. The tip of the electrode is marked by a circle of radius Er, which represents the maximal range of error. This error is further discussed below.

Determination of Concrete Parameters and Program Operation

(1) For simulating various penetrations from which one can select any preferred tract or alternatively drive a microelectrode accurately towards preselected sites within the MGB, we do the following:

(1a) A temporary reference needle is stereotaxically inserted into the brain perpendicular to the horizontal plane ($Y = 0$), and parallel to the coronal and saggital planes ($Z = 0$, $X = 0$, respectively) so that its tip coordinates are

defined. A reference microelectrode is inserted at any arbitrary point within the manipulator plane.

(1b) With the aid of lateral and frontal X-ray views of the reference needle and microelectrode within the brain, we obtain ϕ and θ. The point (X_{tr}, Y_{tr}, Z_{tr}) is evaluated by measuring its X, Y and Z distances from the tip of the reference needle, as both points appear in the two X-ray views, and the reference needle's tip stereotaxic coordinates are known. R is read on the depth scale of the manipulator.

(1c) We try several triplets, each defining a penetration site within the manipulator plane and a depth of a hypothetical microelectrode (u, v and R, respectively). Any triplet is employed for describing graphically the electrode within a section of the simulated MGB in the electrode plane, the latter being defined by the angle γ; e.g., when the microelectrode is perpendicular to the $Y = 0$ plane (horizontal plane), $\gamma = 90°$ represents a coronal section and $\gamma = 0°$ represents a saggital section. From such a set of figures we select, for the actual penetration procedures, those triplets which result in the desired target.

(1d) When the exact stereotaxic coordinates (X_t; Y_t; Z_t) of a certain required target are known we operate the program in the manner described in 2.2 of "program flow".

(2) For identifying the actual recording sites after the experiment, we do the following:

(2a) At the end of the last recording session we make a marker lesion at the tip of the microelectrode defined by a certain triplet (u, v, R), the stereotaxic coordinates of the lesion (X'_t; Y'_t; Z'_t) being determined from histological sections.

(2b) With the aid of these stereotaxic coordinates we can make the proper corrections for the estimated coordinates of the reference microelectrode tip (see 1b):

$$\begin{aligned} X'_{tr} &= X_{tr} + (X'_t - X_t), \\ Y'_{tr} &= Y_{tr} + (Y'_t - Y_t), \\ Z'_{tr} &= Z_{tr} + (Z'_t - Z_t). \end{aligned} \qquad [13]$$

(2c) This information allows the re-execution of the procedures described in 1c, thus providing us with an accurate reconstruction of the recording sites.

Error Estimation

There are various sources of local errors which contribute to the global error in the estimation of the microelectrode tip location (X_t, Y_t, Z_t).

(a) The program employs an approximation of the contour lines of the MGB and its subdivisions, derived from atlas and histological studies. The magnitude of the approximation error is strictly dependent upon the accuracy of these sources, and will decrease as more histological works are published. This limitation holds, of course, for any computer program for modelling any

part of the brain. Errors due to variations between animals may be reduced by applying simple scaling transformations to the coordinates file if we can estimate the specific variation based on X-ray views or other measurements.

(b) Some errors are introduced by inaccurate estimation of the parameters, thus the values actually entered are $R + \Delta R$, $\phi + \Delta\phi$, $\theta + \Delta\theta$, $(X_{tr}, Y_{tr}, Z_{tr}) + \Delta XYZ$. R is read on the micromanipulator depth scale, and ΔR is the maximal resolution of this scale. All of the other parameters are obtained from two X-ray views (lateral and frontal) and errors are introduced due to deviation from the exact position of the X-ray instrumentation. It must be emphasized that the correction procedure described by [13] eliminates the ΔXYZ error since the corrected coordinates are obtained from a marking lesion.

Global error is easily estimated by comparing the value of (X_t, Y_t, Z_t) obtained by Eqs. [1] to [5] to the value of (X_t, Y_t, Z_t) produced by these equations when using $R + \Delta R$, $\phi + \Delta\phi$, etc. Several values of the global error (assuming $\Delta XYZ = 0$) for various parameters are presented in Table II.

In a series of experiments carried out in our laboratory, the parameters were $\Delta R = 0.1$ mm (the resolution of our micromanipulator), and $0° \leq \phi, \theta \leq 20°$. If $\Delta\phi$ and $\Delta\theta$ less than 2°, then the global error is less than $\Delta XYZ + 0.18$ mm. The plots presented in this work were made *after* the determination of the corrected (Xt_r, Yt_r, Zt_r) from lesions, but the radius of the "error circle" was kept as it was during the experiments (before the corrections): 0.25 mm, in order to gain a larger "safety margin." While using the program in the manner described by (1c) we had clear physiological evidence (i.e., single cells responses) that the global error *including* ΔXYZ was also bounded by 0.25 mm.

TABLE II

MAXIMAL ERROR MAGNITUDES (EXCLUDING ΔXYZ) IN mm FOR VARIOUS $\phi,\theta,\Delta\phi,\Delta\theta$[a]

ϕ \ θ	0	20	40	60	80
0	0.08	0.07	0.08	0.1	0.12
	0.16	0.14	0.17	0.21	0.24
20	0.07	0.09	0.11	0.13	0.14
	0.16	0.18	0.22	0.26	0.29
40	0.1	0.1	0.12	0.14	0.16
	0.2	0.21	0.24	0.28	0.33
60	0.11	0.1	0.1	0.12	0.18
	0.22	0.2	0.2	0.24	0.38
80	0.09	0.07	0.07	0.09	0.10
	0.19	0.15	0.14	0.19	0.20

[a] Values in each entry: Upper—for $\Delta\phi$ and $\Delta\theta$ less than 1°; Lower—$\Delta\phi$ and $\Delta\theta$ less than 2°. $R = 20$ mm, $\Delta R = 0.1$ mm.

ACKNOWLEDGMENTS

The authors wish to express their thanks to Professor P. Teitelbaum and Professor E. Kochva for reading and commenting on the manuscript, to Mr. O. D. Comay for help in writing the computer program, to Mr. Z. Schafer for preparing the figures, and to the photography unit of the Zoology Department.

REFERENCES

1. NEWMAN, J. D., AND WOLLBERG, Z. Multiple coding of species specific vocalizations in the auditory cortex of squirrel monkeys. *Brain Res.* **54**, 287–304 (1973).
2. ALLON, N., AND WOLLBERG, Z. Responses of cells in the superior colliculus of the squirrel monkey to auditory stimuli. *Brain Res.* **159**, 78, 321–330 (1978).
3. JORDAN, H. The structure of the medial geniculate nucleus (MGN): A cyto-and myeloarchitectonic study in the squirrel monkey. *J. Comp. Neur.* **148**, 469–480 (1973).
4. BURTON, H., AND JONES, E. G. The posterior thalamic region and its cortical projection in new world and old world monkeys. *J. Comp. Neur.* **168**, 249–302 (1976).
5. ALLON, N., AND WOLLBERG, Z. Responses of cells in the medial geniculate body (MGB) of squirrel monkey to auditory stimuli. *Neuroscience Letters.* Abstracts of the 2nd ENA meeting. Suppl. 1, S2 (1978).
6. BERTRAND G., OLIVER, A. AND THOMPSON, C. J. Computer display of stereotaxic brain maps and probe tracts. *Acta Neurochirurgica Suppl.* **21**, 235–243 (1974).
7. THOMPSON, C. J., HARDY, T., AND BERTRAND, G. A system for anatomical and functional mapping of the human thalamus. *Comput. Biomed. Res.* **10**, 9–24 (1977).
8. HAWRYLYSHYN, P. A., TASKER, R. R., AND ORGAN, L. W. CAAS: Computer-Assisted stereotaxic surgery. *In* Computer Graphics. A Quarterly Report of Siggraph–ACM," Vol. 11, 2, pp. 3–17, 1977.
9. CHRISTIANSEN, H. N., AND SEDERBERG, T. W. Conversion of complex contour line definitions into polygonal element mosaics. *In* "Computer Graphics. A Quarterly Report of Siggraph–ACM," Vol. 12, 3, pp. 187–192, 1978.
10. EMMERS, R., AND AKERT, K. "A Stereotaxic Atlas of the Brain of the Squirrel Monkey (*Saimiri sciureus*)." The University of Wisconsin Press, Madison, Wisc., 1963.